Productions of hadrons, pentaquarks Θ^+ and Θ^{*++}, and di-baryon $(\Omega\Omega)_{0^+}$ in relativistic heavy ion collisions by a quark combination model

Feng-lan Shao,[1,2] Qu-bing Xie,[3,1] and Qun Wang[4,5]
[1]*Department of Physics, Shandong University, Jinan, Shandong 250100, People's Republic of China*
[2]*Department of Physics, Qufu Normal University, Qufu, Shandong 273165, People's Republic of China*
[3]*China Center of Advanced Science and Technology (World Lab), P.O. Box 8730, Beijing 100080, People's Republic of China*
[4]*Institut für Theoretische Physik, J.W. Goethe-Universität, D-60054 Frankfurt/Main, Germany*
[5]*Department of Modern Physics, University of Science and Technology of China, Hefei, Anhui 230026, People's Republic of China*
(Received 9 September 2004; published 21 April 2005)

The hadron production in relativistic heavy ion collisions is well described by the quark combination model. The mixed ratios for various hadrons and the transverse momentum spectra for long-life hadrons are predicted and agree with recent Relativistic Heavy Ion Collider data. The production rates for the pentaquarks Θ^+ and Θ^{*++} and the di-baryon $(\Omega\Omega)_{0^+}$ are estimated, neglecting the effect from the transition amplitude for constituent quarks to form an exotic state.

DOI: 10.1103/PhysRevC.71.044903 PACS number(s): 13.87.Fh, 12.38.Bx, 12.40.−y

I. INTRODUCTION

Recently, a lot of data for hadron multiplicities have been published from the Relativistic Heavy Ion Collider (RHIC) at Brookhaven National Laboratory [1–8]. One purpose of this experiment is to produce a deconfined phase of quarks and gluons (or a quark-gluon plasma, QGP) under extreme conditions at high temperature and density by smashing two gold nuclei. Thus it is important to find reliable probes to judge if the QGP is really formed in the experiment, which is both a theoretical and an experimental challenge because one can detect the free quarks and gluons only indirectly through their decay products. Hadron multiplicities and their correlations are observables encoding information on chemical properties of the medium generated from the heavy ion collisions. It is impressive that the statistical thermal models provide a good description of the available multiplicity data at almost all energies in heavy ion collisions by only a few parameters [9–21]. Although the ability to reproduce the mixed-particle ratio from statistical models is not proof that the emitting source is in thermal equilibrium [21], it is further evidence that such a state, which is one of the necessary conditions for creation of a QGP, has been created. The recombination or coalescence models [22–29] are very successful in explaining the RHIC puzzles [30–35], e.g., an anomaly in the ratio of proton to pion that is unexpectedly high (reaching about 1) at the middle transverse momentum region. This implies that the hadronization by quark recombination plays an important role even in the hard regime characterized by high transverse momenta and provides a piece of evidence for deconfinement (see, e.g., [36]).

The earliest quark combination model (QCM) dates back to the 1970s [37,38], when it was proposed to describe the multiparticle production or the hadronization in various reactions. Certainly the most popular hadronization models nowadays are the string and the cluster model [39–41], but the great advantage of the quark combination picture in describing the inclusive hadron production is its simplicity. The success of the QCM in almost all kinds of high-energy collisions, e.g., electron-positron, hadron-hadron, and nucleus-nucleus collisions, is partly due to the universal stochastic nature of fragmentation or hadronization. In this sense, the QCM resembles the thermal or the statistical model, but it encodes more microscopic information.

We have developed a variant of the QCM based on a simple quark combination rule [42,43]. Using our QCM, we have described most of the multiplicity data for hadrons in electron-positron and proton-proton/antiproton collisions [44–50]. Also, we solved a difficulty facing other QCMs in describing the TASSO data for the baryon-antibaryon correlation: they can be successfully explained by our QCM [43,51]. Embedded in the event generator, our QCM can also reproduce most of the global properties of hadronic events such as momentum spectra in electron-positron collisions [52–56]. Encouraged by the success of the statistical and recombination models in heavy ion collisions, we try in this paper to extend our QCM to reproduce the recent RHIC data for hadron multiplicities. Especially, we will predict the production rates of three exotic baryons: the pentaquarks Θ^+ and Θ^{*++} and the di-baryon $(\Omega\Omega)_{0^+}$.

The pentaquark Θ^+ is an exotic baryon made of five quarks $uudd\overline{s}$, which were discussed in the context of quark models in the early days of QCD [57,58]. In 1997, Diakonov *et al.* [59] predicted the mass and width of Θ^+ at about 1540 and 15 MeV, respectively, using the chiral soliton model. Recent work on the property of the pentaquark in the chiral field model can be found, e.g., in Refs. [60–62]. Several experimental groups have reported the discovery of the pentaquark state Θ^+ [63–67]. Another pentaquark Θ^{*++} belongs to the 27-plet baryon with flavor content $uuud\overline{s}$ and possible spin-parity $J^P = (3/2)^+$ [61]. A search for the Θ^{*++} pentaquark has been carried out by the BABAR Collaboration [68] in the decay channel $B^\pm \to p\overline{p}K^\pm$, but the results in this experiment are preliminary and yet to be confirmed. The last exotic state we are going to look at is the di-baryon $(\Omega\Omega)_{0^+}$. For more than 20 years, the search for a di-baryon has been another important attempt in hadronic physics [69–74]. One believes that if di-baryons do exist, those with multistrangeness must be ideal candidates to observe because of their relatively long lifetime due to their stability with respect to strong decay. Recently, the structure and properties of di-baryons with large strangeness were investigated in the chiral SU(3) model [75–78], which quite successfully reproduces several nuclear properties. They found that some six-quark states with high strangeness have considerable binding energy provided by the chiral quark coupling. Of particular interest is $(\Omega\Omega)_{0^+}$. It is a deeply bound state (binding energy is around 100 MeV; the mean-square root of the distance between two Ω's is 0.84 fm). The mean lifetime of this di-baryon is about twice that of Ω, because it only decays weakly. All these interesting properties, together with the electric charge $Q=-2$, would make it easily identified in the experiments. Because of its large strangeness, $(\Omega\Omega)_{0^+}$ is not likely to be produced in proton-proton collisions. However, one expects enhanced strangeness production [14–16] in heavy ion collisions at RHIC energies, which can be the best place to study the production of the di-baryon $(\Omega\Omega)_{0^+}$ [79,80].

The outline of this paper is as follows. In Secs. II and III, we give a brief description of the quark combination model and basic relations among production weights of $SU_f(3)$ multiplets. In Sec. IV we present particle ratios and the transverse momentum spectra of the pion, proton, and kaon predicted from the quark combination model. The upper limits for production rates of Θ^+ and $(\Omega\Omega)_{0^+}$ are estimated in Secs. V and VI. We give a summary of results and conclusions in Sec. VII.

II. THE QUARK COMBINATION MODEL

All kinds of hadronization models demand that they satisfy rapidity or the momentum correlation for quarks in the neighborhood of phase space. The essence of this correlation is its agreement with the fundamental requirement of QCD which uniquely determines the quark combination rule (QCR) [43]. According to QCD, a $q\overline{q}$ may be in a color octet or a singlet, which means there is a repulsive or an attractive interaction between them. The smaller the difference in rapidity for two quarks, the longer is the interaction time. So there is enough time for a $q\overline{q}$ to be in a color singlet and form a meson. Similarly, a qq can be in a sextet or an antitriplet. If its nearest neighbor is a q in rapidity, they form a baryon. If the neighbor is a $\overline{q}$, because the attraction strength of the singlet is two times that of the antitriplet, $q\overline{q}$ will win the competition to form a meson and leave a q alone. Our quark combination model is based on the above QCD requirements. When the transverse momenta of quarks are negligible, all q and $\overline{q}$ can always line up stochastically in rapidity. The QCR reads as follows:

1. Start from the first parton (q or $\overline{q}$) in the line.
2. If the baryon number of the second parton in the line is of a different type from the first, i.e., the first two partons are either $q\overline{q}$ or $\overline{q}q$, they combine into a meson and are removed from the line, go back to point 1; otherwise they are either qq or $\overline{qq}$, go to point 3.
3. Look at the third parton. If it is of a different type from the first, the first and third partons form a meson and are removed from the line, go back to point 1; otherwise, the first three partons combine into a baryon or an antibaryon and are removed from the line, go back to point 1.

Here is an example of how the above QCR works. All partons line up in rapidity and combine to hadrons as follows:

$$
\begin{aligned}
&q_1\overline{q}_2\overline{q}_3\overline{q}_4\overline{q}_5q_6\overline{q}_7q_8q_9q_{10}\overline{q}_{11}q_{12}q_{13}q_{14}\overline{q}_{15}q_{16}q_{17}\overline{q}_{18}\overline{q}_{19}\overline{q}_{20}\\
&\to M(q_1\overline{q}_2)\ \overline{B}(\overline{q}_3\overline{q}_4\overline{q}_5)\ M(q_6\overline{q}_7)\ B(q_8q_9q_{10})\ M(\overline{q}_{11}q_{12})\\
&\times M(q_{13}\overline{q}_{15})\ B(q_{14}q_{16}q_{17})\ \overline{B}(\overline{q}_{18}\overline{q}_{19}\overline{q}_{20}),
\end{aligned}
\tag{1}
$$

We note that it is straightforward to define the QCR in one-dimensional phase space, but it is more complicated to have it in two- or three-dimensional phase space, where one does not have an order or one has to define an order in a sophisticated way so that all quarks can combine to a hadron in a particular sequence; see, for example, Ref. [81].

If the quarks and antiquarks are stochastically arranged in rapidity, the probability distribution for N pairs of quarks and antiquarks to combine into M mesons, B baryons, or B antibaryons is

$$X_{MB}(N)=\frac{2N(N!)^2(M+2B-1)!}{(2N)!M!(B!)^2}3^{M-1}\delta_{N,M+3B}. \tag{2}$$

The average numbers of primarily produced mesons $M(N)$ and baryons $B(N)$ are given by

$$\langle M(N)\rangle=\sum_M\sum_B MX_{MB}(N), \tag{3}$$

$$\langle B(N)\rangle=\sum_M\sum_B BX_{MB}(N). \tag{4}$$

Approximately, for $N\geqslant 3$, $\langle M(N)\rangle$ and $\langle B(N)\rangle$ can be well parametrized as linear functions of quark number N: $\langle M(N)\rangle=aN+b$ and $\langle B(N)\rangle=(1-a)N/3-b/3$, where $a=0.66$ and $b=0.56$. However, for $N<3$, one obviously has $\langle M(N)\rangle=N$ and $\langle B(N)\rangle=0$.

Having the number of mesons and baryons in an event, we can obtain the multiplicity of all primary hadrons from their production weights. The yield of the hadron h_i can be written as

$$
\begin{aligned}
\langle h_i\rangle=&\sum_j C_{M_j}\langle M\rangle\mathrm{Br}(M_j\to h_i)+\sum_j C_{B_j}\langle B\rangle\mathrm{Br}(B_j\to h_i)\\
&+\sum_j C_{\overline{B}_j}\langle B\rangle\mathrm{Br}(\overline{B}_j\to h_i),
\end{aligned}
\tag{5}
$$

where $\langle M\rangle$ and $\langle B\rangle$ are the average number of mesons and baryons, respectively. C_{M_j}, C_{B_j}, and $C_{\overline{B}_j}$ are the normalized weights for the primary meson M_j, the primary baryon B_j, and the primary anti baryon $\overline{B}_j$, respectively. Obviously we have the property $C_{B_j}=C_{\overline{B}_j}$, and $\mathrm{Br}(h_j\to h_i)$ is the weighted branching ratio for h_j to h_i.

The production weights C_{M_j} and C_{B_j} for primary hadrons satisfy the $SU_f(3)$ symmetry with a strangeness suppression factor λ_s for strange hadrons [82–84]. To determine C_{M_j} and C_{B_j}, we need the ratio V/P of the vector ($J^P=1^-$) to the pseudoscalar ($J^P=0^-$) meson, and the ratio $(3/2)^+/(1/2)^+$ of the decouplet $[J^P=(3/2)^+]$ to the octet $[J^P=(1/2)^+]$ baryon. Assuming SU(6) symmetry, Anisovich *et al.* [37] gave

TABLE I. The weights of quark combination and those in terms of baryon multiplets.

Flavor content	Combination weight	Production weight of baryon multiplets
uuu	1	P_{10}
ddd	1	P_{10}
sss	λ^3	$P_{10}\lambda^3$
uud	3	$P_{10} + P_8$
uus	3λ	$[P_{10} + P_8]\lambda$
ddu	3	$P_{10} + P_8$
dds	3λ	$[P_{10} + P_8]\lambda$
uss	$3\lambda^2$	$[P_{10} + P_8]\lambda^2$
dss	$3\lambda^2$	$[P_{10} + P_8]\lambda^2$
uds	6λ	$[P_{10} + 2(P_8 + P_{1'})]\lambda$

$V/P = 3$. In this case, the weights for all mesons except η and η' can be simply written as $C_{M_i} \propto (2J_i + 1)\lambda_s^{r_i}$, where J_i is the spin of M_i, and r_i is the number of strange quarks and/or antiquarks in the meson. However, there is a spin suppression effect associated with baryons. In the next section, we derive the two relations between the production weights for octet, decuplet, and singlet baryons from the properties of hadronization in the quark combination scheme.

III. SU$_f$(3) SYMMETRY AND FLAVOR CONSERVATION IN THE QCM

Hadronization is the soft process of the strong interaction and is independent of flavor, so the net flavor number remains constant during the process, which we call the property of flavor conservation. In the quark combination scheme, this means that the number of quarks of a certain flavor prior to hadronization equals that of all the primarily produced hadrons after it. The λ_s-broken SU$_f$(3) symmetry in hadron production means baryons or mesons in the same J^{PC} multiplet share an equal production rate up to a λ_s^r factor. This SU$_f$(3) symmetry has been supported by many experiments, particularly by the fact that the observed λ_s obtained from various mesons and baryons coincide with one another [82]. This experimental fact is unexpected in the usual diquark model for baryon production and turns out to be in favor of the quark combination scheme [85] in which a baryon is formed by the stochastic combination of three constituent quarks.

From the above properties, we can obtain relations among the production weights for octet, decuplet, and singlet baryons in the quark combination picture [46]. In Table I, all the flavor combinations are listed in the first column, with their combination weights in the second. In hadronization, three quarks combine into a primary baryon which satisfies the λ_s-broken SU$_f$(3) symmetry. Each flavor combination in the first column corresponds to a certain baryon belonging to several SU$_f$(3) multiplets, whose production weight is listed in the third column. The ground-state decuplet and octet baryons are denoted by 10 and 8, while the only excited baryon that we consider, the singlet $\Lambda(1520)$, is denoted by $1'$. Their corresponding weights are denoted by P_{10}, P_8, and $P_{1'}$ respectively. Noting that the two sets of weights must be associated with a common factor, we finally derive the following relations among the production weights for octet, decuplet, and singlet baryons:

$$P_{10} = P_{1'} \tag{6}$$

$$P_8 = 2P_{10} \tag{7}$$

They impose a global constraint on the production rates of all ground-state baryons and the excited singlet baryon $\Lambda(1520)$. We can understand the so-called spin suppression from the basic relations. For those decuplet and octet baryons that are primarily produced and have the same strangeness, the ratio of their production rate is

$$R = \frac{(3/2)^+}{(1/2)^+} = \frac{P_{10}}{P_8} = 0.5. \tag{8}$$

Note that the ratio R measured in experiments is for the octet baryons, which include decay products from the decuplet ones. We then obtain the following approximated value for $R_{\rm exp}$ when neglecting the production of excited baryons:

$$R_{\rm exp} = \frac{(3/2)^+(\text{ground})}{(1/2)^+(\text{ground})} \sim \frac{P_{10}}{P_{10} + P_8} \sim 0.3. \tag{9}$$

Note that $R_{\rm exp}$ is much less than 2 from spin counting, which is called the spin suppression effect.

We can see that there is an essential difference between the spin suppression factor R for the baryon and the multiplicity ratio of vector mesons to pseudoscalar mesons V/P. The former is for the ratio of the $(3/2)^+$ decuplet baryon to the $(1/2)^+$ octet one. They belong to different SU$_f$(3) multiplets. The basic relations impose a constraint upon their production weights. The latter is the ratio of vector to pseudoscalar mesons, both of which belong to SU$_f$(3) nonets. Flavor conservation and SU$_f$(3) symmetry hold in each nonet and hence there is no restriction on their weights.

IV. HADRON MULTIPLICITIES AND MOMENTUM SPECTRA

In this section, we use the QCM to compute hadron multiplicities and their ratios in heavy ion collisions at RHIC energies. We will also calculate the transverse momentum spectra for pions, kaons, and protons. Before we do that, we have to determine some input parameters of the QCM. The parameters which control the total multiplicity are the number of quarks and antiquarks. In electron-positron and proton-antiproton collisions, the number of quarks is equal to that of antiquarks, which means there are no excess baryons in contrast to antibaryons. For nucleus-nucleus collisions, however, we need two parameters, the number of quarks and antiquarks, to account for the net baryon number even in central rapidity. These two parameters are determined by fitting the the total charged multiplicity data, $\langle N_{\rm ch}\rangle_{\rm data} = 4100 \pm 210$, in central Au + Au collisions at 130 A GeV [1], which corresponds to the total number of quarks and antiquarks $\langle N_q + N_{\bar{q}}\rangle = 7400$ in the QCM. The quark number $\langle N_q\rangle$ and the antiquark number $\langle N_{\bar{q}}\rangle$ can be further determined by the ratio of

TABLE II. Antiparticle to particle ratios. Our QCM predictions and STAR data at 130 [3] and 200 [4] A GeV.

	STAR (130 A Gev)	QCM (130 A Gev)	STAR (200 A Gev)	QCM (200 A Gev)
$\overline{p}/p$	$0.71 \pm 0.01 \pm 0.04$	0.71	0.73 ± 0.05	0.78
$\overline{\Lambda}/\Lambda$	$0.71 \pm 0.01 \pm 0.04$	0.79	0.84 ± 0.05	0.84
$\overline{\Xi}^+/\Xi^-$	$0.83 \pm 0.04 \pm 0.05$	0.88	0.94 ± 0.08	0.91
$\overline{\Omega}^+/\Omega^-$	$0.95 \pm 0.15 \pm 0.05$	1.00	1.03 ± 0.12	1.00

antiproton to proton $\overline{p}/p = 0.7$ [3,4]. Then we obtain $\langle N_q \rangle = 3920$ and $\langle N_{\overline{q}} \rangle = 3500$, where we see that the net quark number is about 420. Another parameter is the strangeness suppression factor λ_s which has also to be input from data. We find $\lambda_s = 0.5$ is consistent with data $\Phi/K^{*0} = 0.47$ [2]. At 200 A GeV, we determine in the same way the total number of quarks and antiquarks $\langle N_q + N_{\overline{q}} \rangle = 8900$ with the net quark number 360 and $\lambda_s = 0.6$ by fitting the data [86].

Having determined the above parameters, we calculate the ratios of strange antibaryons to their baryon counterparts, $\overline{\Lambda}/\Lambda$, $\overline{\Xi}^+/\Xi^-$, and $\overline{\Omega}^+/\Omega^-$, in midrapidity of central Au + Au collisions and compare our results with STAR data [3,4]. The above antibaryon to baryon ratios are mainly controlled by the net quark number from colliding nucleons. The results are listed in Table II. The data show that the ratios increase with strangeness of the baryons. The reason for this trend is that the quark pair production is more important than the baryon transport in midrapidity. We see that there is good agreement between our model predictions and the data, which means the quark combination mechanism can explain this behavior. In the QCM, various ratios $\overline{B}/B$ are associated with a common multiplicative factor D which is given by the ratio K^+/K^-, for example, $\overline{\Lambda}/\Lambda = D(\overline{p}/p)$, $\overline{\Xi}/\Xi = D(\overline{\Lambda}/\Lambda)$, and $\overline{\Omega}/\Omega = D(\overline{\Xi}/\Xi)$. The calculated ratio K^+/K^- and the D factor in these compound ratios are listed in Table III. We also calculate the ratios of single-strange particles to nonstrange particles and those of multistrange particles to single-strange particles. The results and the experimental data [3–5] are given in Tables IV and V. All the above show that the mixed ratios for various hadrons agree with RHIC data.

As a test of our QCM, we finally calculate the transverse momentum spectra for the pion, kaon, and proton. Two steps are needed to determine the final hadron spectra. One is to obtain the spectra for initially produced hadrons, which are those before their decay. We can do this through our quark combination model. The next step is to let these initially produced hadrons decay to final-state hadrons, which are observed in experiments. In our QCM, the longitudinal momentum is described by the constant distribution of rapidity, where we assume that quarks and antiquarks are distributed in the rapidity range $y \in [-2.8, 2.8]$ at 130 GeV and $y \in [-3.0, 3.0]$ at 200 GeV with equal probability. This corresponds to the rapidity distribution of charged multiplicity at RHIC. Once the transverse momentum and rapidity for each quark are determined, their momenta are fixed. We can randomly line up all quarks in rapidity and let them combine into hadrons following the combination rule in Sec. II. The momentum of a hadron is then the sum of that of its constituent quarks, while its energy is given by the mass-shell condition. The transverse momentum distribution of quark or antiquark is extracted from the measured neutral pion spectra at 200 A GeV [87], where we assume that they are identical because the observed ratios of antiparticles to particles, i.e., $\overline{p}/p$, $\overline{\Lambda}/\Lambda$, $\overline{\Xi}^+/\Xi^-$, and K^+/K^-, are almost constant with p_T [3]. This is what we get for quark or antiquark p_T distribution: $f(p_T) = (p_T^{2.3} + p_T^{0.2} + 1)^{-3.0}$. We assume that the combination occurs only among those constituent quarks having the same azimuthal angle, similar to the strategy in Ref. [22]. Note that all these hadrons after combination are primarily produced; in order to get the spectra comparable to the data, one has to let them decay in their center-of-mass system. The momenta of all decayed hadrons are then boosted back into the laboratory frame and recorded. Here we make use of the approriate function of the event generator JETSET [88]. Finally we obtain the p_T spectra for the pions, kaons, and protons in the final state, which includes all contributions from decay.

That we distinguish primarily produced hadrons from the final-state ones marks the *essential difference* between our model and other recombination or coelescence models [22–29], where that distinction is not made. Just to get the feeling of this substantial difference, one may take pions

TABLE III. K^+/K^- ratio compared with compound ratios of baryons at 130 A GeV [3].

	STAR	QCM
K^+/K^-	1.092 ± 0.023	1.122
$\frac{\overline{\Lambda}/\Lambda}{\overline{p}/p}$	0.98 ± 0.09	1.10
$\frac{\overline{\Xi}^+/\Xi^-}{\overline{\Lambda}/\Lambda}$	1.17 ± 0.11	1.11
$\frac{\overline{\Omega}^+/\Omega^-}{\overline{\Xi}^+/\Xi^-}$	1.14 ± 0.21	1.15

TABLE IV. A group of ratios for strange hadrons compared with STAR data at 130 A GeV [3–5].

	STAR	QCM
Φ/K^*0	$0.49 \pm 0.05 \pm 0.12$	0.47
K^+/π^-	$0.161 \pm 0.002 \pm 0.024$	0.146
K^-/π^-	$0.146 \pm 0.002 \pm 0.022$	0.130
$(\overline{\Omega}^+ + \Omega^-)/h^-$	$(2.24 \pm 0.69) \times 10^{-3}$	3.21×10^{-3}

TABLE V. A group of ratios for strange hadrons compared with STAR data at 200 A GeV [7,8].

	STAR	QCM
K^-/π^-	0.146 ± 0.024	0.132
$\overline{p}/\pi^-$	0.09 ± 0.01	0.089
Ω^-/h^-	$(1.20 \pm 0.12) \times 10^{-3}$	1.40×10^{-3}
π^-/π^+	$1.025 \pm 0.006 \pm 0.018$	1.008
K^-/K^+	$0.95 \pm 0.03 \pm 0.03$	0.92

as an example: even in the range $p_T > 2\,\mathrm{GeV}/c$, about 70% of pions come from resonance decays. This is why our quark p_T spectrum extracted from data decreases not exponentially at low transverse momenta but in a power law—*it reflects the spectra of initially produced hadrons instead of final-state ones*. Another difference between our model and other combination models is that the quark p_T distribution is given by a single function without distinguishing between thermal quarks (low p_T) and shower quarks (high p_T). In any combination models, the role of gluons is finally taken by quark-antiquark pairs; for example, shower quarks are developed after a QCD cascade. In our QCM, the number of constituent quarks already effectively includes those quark-antiquark pairs converting from gluons. All quarks in the whole p_T range are assumed to combine following the same combination rule. This assumption is widely used in other combination models: combination among shower quarks is treated in the same way as that among thermal quarks. The difference just lies in the sources: shower quarks are products after QCD showering, whereas thermal quarks arise from thermal distribution. Except for these differences, our model is basically the same as other combination models. For example, the rapidity correlation principle in our model is also implied in other models. Hwa-Yang's model [22] assumes $y_1 = y_2 = y_h$ and $(y_1 + y_2)/2 = y_h$, where y_1 and y_2 are quark rapidities, and y_h is the hadron one; whereas the GKL model [24] uses the even simpler assumption that $y_1 = y_2 = y_h = 0$.

Instead of predicting the p_T spectra, we give the spectra of the scaling variable $z = p_T/K$, where the scaling factor K is defined in Ref. [22]. The result for pions, kaons, and protons at 130 and 200 A GeV are shown in Figs. 1–3. We see that the agreement between our predictions and the data is quite satisfactory and that we have verified the perfect scaling behavior in our model. Moreover, the observed enhancement of protons and antiprotons at intermediate transverse momenta [6] can be naturally explained because we have the right predictions for protons.

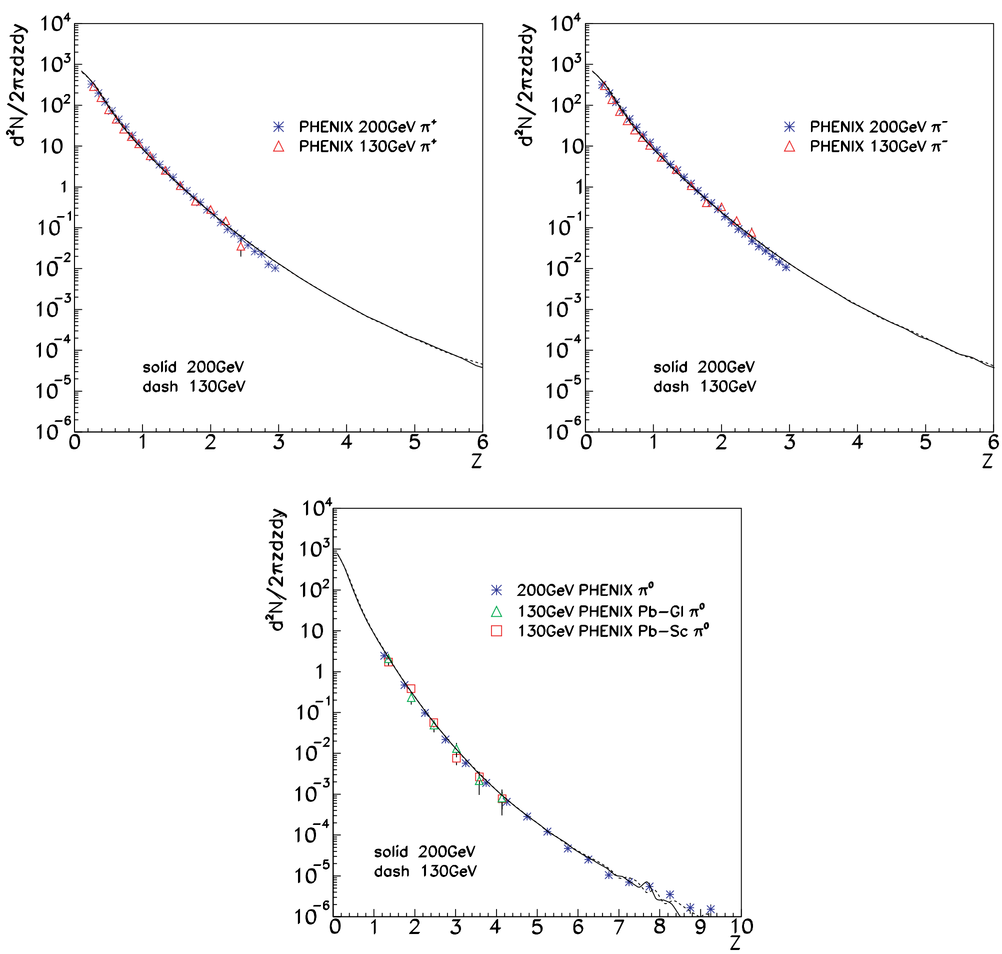

FIG. 1. (Color online) The spectra in p_T scaling variable $z = p_T/K$ (K is the scaling factor) for $\pi^\pm$ and π^0 in the 5% and 10% most central collisions at 130 and 200 A GeV, respectively. The solid and dashed lines are our results. The data are from PHENIX.

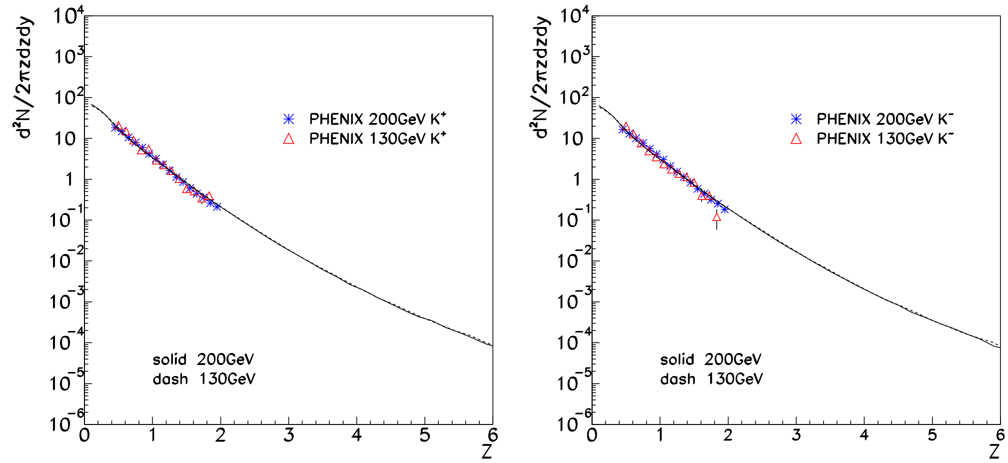

FIG. 2. (Color online) The same spectra for $K^{\pm}$ in the 5% most central collisions at 130 and 200 A GeV. The solid and dashed lines are our results. The data are from PHENIX.

V. MULTIPLICITIES OF Θ^{+} AND Θ^{*++}

In this section we will give an estimate of the multiplicities of Θ^{+} and Θ^{*++} at 130 and 200 A GeV. Several groups have already predicted the yields of Θ^{+} in central Au + Au collisions by the statistical and coalescence models [89–91].

In the QCM, it is quite easy to estimate the production rate of Θ^{+} and Θ^{*++}. The probabilities $P(uudd\bar{s})$ and $P(uuud\bar{s})$ for five quarks $uudd\bar{s}$ and $uuud\bar{s}$, respectively, to come together in rapidity can be easily obtained by the QCM. The overlapping of phase space (here rapidity) has been encoded in the probability P. Then the probabilities to form the pentaquark Θ^{+} and Θ^{*++} can be estimated by spin counting: a system composed of five quarks, each of which has spin-1/2, has a total 2^5 spin states composed of one spin-5/2, four spin-3/2, and five spin-1/2 states. Assuming that all spin-1/2 states form Θ^{+}, the production rate for Θ^{+} is then $P(\Theta^{+}) = \frac{10}{32}P(uudd\bar{s})$. If all spin-3/2 states go to Θ^{*++}, the production rate of Θ^{*++} is then $P(\Theta^{*++}) = \frac{16}{32}P(uuud\bar{s})$. Note that the current spin-counting method only provides a kind of upper limit for the yields. In the real calculation, one must evaluate the transition probability which involves overlapping the wave functions of pentaquark states and their quark constituents. Here we simplify the problem by assuming the transition amplitude is unity. Also we neglect the contribution from the hadron-hadron rescattering in hadronic phase and assume the dominant source is from quark combination. Our estimates for Θ^{+} and Θ^{*++} are shown in Table VI. At 130 A GeV, about 1.16 Θ^{+} and 1.86 Θ^{*++} per rapidity are produced in midrapidity in central Au + Au collisions, while at 200 A GeV, the yields of Θ^{+} and Θ^{*++} are 1.30 and 2.08 per rapidity, respectively. Our predictions agree with those given by the statistical models [89,90]. For comparison, the yield of Θ^{+} in proton-proton collisions is predicted to be about 10^{-2} to 10^{-3} [92,93].

VI. MULTIPLICITY OF $(\Omega\Omega)_{0+}$

We have calculated the ratios of strange antibaryons to their baryon counterparts and the ratios of Ω to negatively

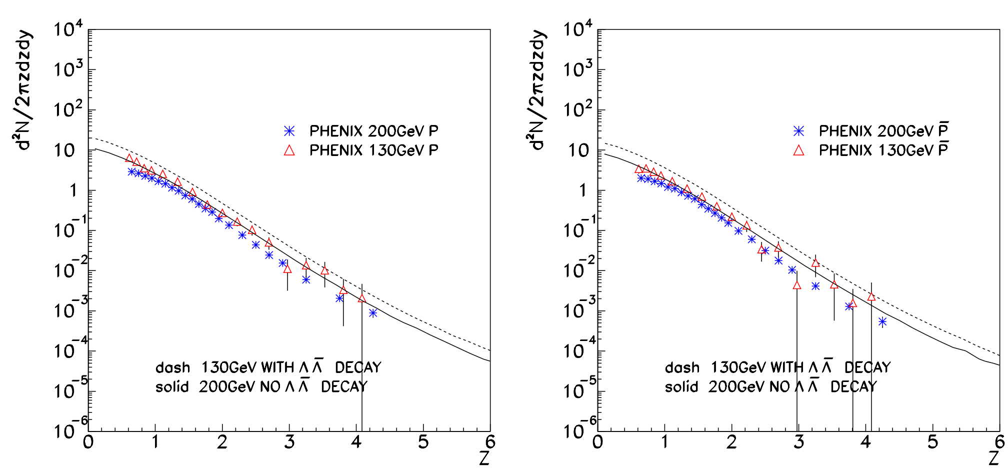

FIG. 3. (Color online) The same spectra for $p, \bar{p}$ in the 5% most central collisions at 130 and 200 A GeV. The solid and dashed lines are our results. The data are from PHENIX.

TABLE VI. Upper limits for multiplicities of Θ^+, Θ^{*++}, and $(\Omega\Omega)_{0^+}$ at 130 and 200 A GeV. Per-event values are obtained by taking the full-rapidity range as $|y| < 3.43$.

	Per rapidity (130 A GeV)	Per event (130 A GeV)	Per rapidity (200 A GeV)	Per event (200 A GeV)
Θ^+	1.16	7.97	1.30	8.93
Θ^{*++}	1.86	12.75	2.08	14.29
Ω^-	0.40	2.74	0.51	3.50
$(\Omega\Omega)_{0^+}$	2.70×10^{-5}	1.86×10^{-4}	3.67×10^{-5}	2.52×10^{-4}
$(\Omega\Omega)_{0^+}/\Omega^-$	6.79×10^{-5}	6.79×10^{-5}	7.20×10^{-5}	7.20×10^{-5}

charged particles. The results are consistent with available data; see Tables IV and V. Based on the results for Ω, we will predict in this section multiplicities of the di-baryon $(\Omega\Omega)_{0^+}$ in Au + Au collisions at 130 and 200 A GeV.

First we estimate the yield of Ω $(\overline{\Omega}^+ + \Omega^-)$. Assuming the ratio of Ω to h^- is constant for all rapidities, we get the yield of Ω per event to be about 5 and 6 from the experimental data $h^- \approx 1/2N_{\mathrm{ch}}^{\mathrm{data}} \approx 2050$ at 130 A GeV [1] and $h^- \approx 1/2N_{\mathrm{ch}}^{\mathrm{data}} \approx 2450$ at 200 A GeV [81], respectively. In the quark combination picture, the production weight for Ω^- is proportional to λ_s^3. We find that the multiplicities increase strongly with growing λ_s, from 0.76 at $\lambda_s = 0.3$ to 6.00 at $\lambda_s = 0.7$. Our predictions for the Ω^- yields are listed in Table VI. Given the result for Ω^-, we are now in a position to estimate the multiplicity of $(\Omega\Omega)_{0^+}$. First we find the probability $P(ssssss)$ for six s quarks to come together under the rule of our QCM and then we apply the spin counting to estimate the yield of $(\Omega\Omega)_{0^+}$. There are a total of 2^6 spin states for a six-quark system. In terms of total spin, these are one spin-3, five spin-2, nine spin-1, and five spin-0 states. We assume that all spin-0 states go to $(\Omega\Omega)_{0^+}$. The yield of $(\Omega\Omega)_{0^+}$ is then $\frac{5}{64}$ times that of six s quarks. The results are shown in Table VI. Same as the results for pentaquarks, the yields of $(\Omega\Omega)_{0^+}$ in Table VI are only regarded as a kind of upper limit because we neglected the effect of the transition amplitude for six s quarks to form a di-Ω. One sees that in an event, the multiplicities of $(\Omega\Omega)_{0^+}$ are about 1.86×10^{-4} at 130 A GeV and 2.52×10^{-4} at 200 A GeV, respectively. Our predictions agree in magnitude with those of the coalescence models [79]. Normally one can detect $(\Omega\Omega)_{0^+}$ through its decay product. Because the binding energy of $(\Omega\Omega)_{0^+}$ is relatively large, which prevents it from strong decay, $(\Omega\Omega)_{0^+}$ mainly decays weakly into one Ω plus the decay products of Ω (three- or more-body decay) or into Ω and Ξ (two-body decay). If it is produced in the experiments, one could detect it through the above decay channels. For other experimental traces of di-baryons, see, for example, Refs. [94,95].

VII. SUMMARY

In this paper, we extend our quark combination model, which is very successful in describing the hadron production in electron-positron and proton-proton(antiproton) collisions, to reproduce the multiplicity data in heavy ion collisions at RHIC energies 130 and 200 A GeV. The model can describe available data for transverse momentum spectra for pions, kaons, and protons; especially, the p_T scaling behavior can be well reproduced within our simple model. It can explain the abnormality of the proton to pion ratio at intermediate transverse momenta. A variety of ratios for antibaryons to baryons, single-strange hadrons to nonstrange ones, and double-strange hadrons to single-strange ones can all be reproduced in our QCM. With the approximation that the transition probability for constituent quarks to form an exotic state is taken as unity if they come together in rapidity according to our combination rule, we finally estimate the yields of Θ^+, Θ^{*++}, and $(\Omega\Omega)_{0^+}$ in Au + Au collisions at 130 and 200 A GeV. These yields can be regarded as a kind of upper limit. The multiplicities of Θ^+ and Θ^{*++} are estimated to be about 1 and 2 per rapidity in midrapidity in a central event, respectively, while the rate of $(\Omega\Omega)_{0^+}$ is of the magnitude 10^{-5} per rapidity. The multiplicities of Θ^+ and Θ^{*++} are found to be almost independent of the strangeness suppression factor λ_s, while that of $(\Omega\Omega)_{0^+}$ increases strongly with growing λ_s.

ACKNOWLEDGMENTS

The authors thank C. R. Ching, S.-Y. Li, Z.-T. Liang, T. H. Ho, Z.-G. Si, F. Wang, Y. W. Yu, and Z.Y. Zhang for helpful discussions. Q. W. thanks K. Redlich for critically reading the manuscript and for many insightful comments. Q.W. acknowledges support by the Virtual Institute VH-VI-041 of the Helmholtz Association of National Research Centers. The work of F.L.S. and Q.B.X. is supported in part by the National Natural Science Foundation of China under Grant No. 10475049 and the University Doctor Point Foundation of China under Grant No. 20030422064.

[1] B. B. Back *et al.*, Phys. Rev. Lett. **91**, 052303 (2003).
[2] C. Adler *et al.* (STAR Collaboration), Phys. Rev. C **66**, 061901 (2002).
[3] J. Adams *et al.* (STAR Collaboration), Phys. Lett. **B567**, 167 (2003).
[4] B. Hippolyte (STAR Collaboration), arXiv:nucl-ex/0306017.
[5] C. Adler *et al.* (STAR Collaboration), Phys. Lett. **B595**, 143 (2004).
[6] K. Adcox *et al.* (PHENIX Collaboration), Phys. Rev. C **69**, 024904 (2004).
[7] B. B. Back *et al.* (PHOBOS Collaboration), Phys. Rev. C **67**, 021901 (2003).

[8] K. Filimonov (STAR Collaboration), arXiv:hep-ex/0306056.
[9] P. Braun-Munzinger, K. Redlich, and J. Stachel, arXiv:nucl-th/0304013.
[10] P. Braun-Munzinger, J. Stachel, and C. Wetterich, arXiv:nucl-th/0311005.
[11] P. Braun-Munzinger, I. Heppe, and J. Stachel, Phys. Lett. **B465**, 15 (1999).
[12] P. Braun-Munzinger, D. Magestro, K. Redlich, and J. Stachel, Phys. Lett. **B518**, 41 (2001).
[13] J. Cleymans and K. Redlich, Phys. Rev. C **60**, 054908 (1999).
[14] J. Rafelski and B. Muller, Phys. Rev. Lett. **48**, 1066 (1982); **56**, 2334(E) (1986).
[15] B. Muller and J. Rafelski, Phys. Lett. **B101**, 111 (1981).
[16] P. Koch, B. Muller, and J. Rafelski, Phys. Rep. **142**, 167 (1986).
[17] G. Torrieri, W. Broniowski, W. Florkowski, J. Letessier, and J. Rafelski, arXiv:nucl-th/0404083.
[18] G. Torrieri and J. Rafelski, J. Phys. G **30**, S557 (2004).
[19] E. L. Bratkovskaya, W. Cassing, C. Greiner, M. Effenberger, U. Mosel, and A. Sibirtsev, Nucl. Phys. **A675**, 661 (2000).
[20] B. Schenke and C. Greiner, J. Phys. G **30**, 597 (2004).
[21] D. H. Rischke, Nucl. Phys. **A698**, 153 (2002).
[22] R. C. Hwa and C. B. Yang, Phys. Rev. C **67**, 034902 (2003).
[23] R. C. Hwa and C. B. Yang, Phys. Rev. C **70**, 024905 (2004).
[24] V. Greco, C. M. Ko, and P. Levai, Phys. Rev. Lett. **90**, 202302 (2003).
[25] V. Greco and C. M. Ko, arXiv:nucl-th/0405040.
[26] V. Greco, C. M. Ko, and P. Levai, Phys. Rev. C **68**, 034904 (2003).
[27] R. J. Fries, B. Muller, C. Nonaka, and S. A. Bass, Phys. Rev. Lett. **90**, 202303 (2003).
[28] C. Nonaka, R. J. Fries, and S. A. Bass, Phys. Lett. **B583**, 73 (2004).
[29] R. J. Fries, B. Muller, C. Nonaka, and S. A. Bass, Phys. Rev. C **68**, 044902 (2003).
[30] K. Adcox *et al.* (PHENIX Collaboration), Phys. Rev. Lett. **88**, 022301 (2002).
[31] C. Adler *et al.* (STAR Collaboration), Phys. Rev. Lett. **90**, 082302 (2003).
[32] K. Adcox *et al.* (PHENIX Collaboration), Phys. Rev. Lett. **88**, 242301 (2002).
[33] C. Adler *et al.* (STAR Collaboration), Phys. Rev. Lett. **86**, 4778 (2001); **90**, 119903(E) (2003).
[34] C. Adler *et al.* (STAR Collaboration), Phys. Rev. Lett. **89**, 092301 (2002).
[35] K. Adcox *et al.* (PHENIX Collaboration), Phys. Rev. Lett. **89**, 092302 (2002).
[36] U. W. Heinz, arXiv:nucl-th/0407067.
[37] V. V. Anisovich and V. M. Shekhter, Nucl. Phys. **B55**, 455 (1973).
[38] J. D. Bjorken and G. R. Farrar, Phys. Rev. D **9**, 1449 (1974).
[39] B. Andersson, G. Gustafson, G. Ingelman, and T. Sjostrand, Phys. Rep. **97**, 31 (1983).
[40] B. R. Webber, Nucl. Phys. **B238**, 492 (1984).
[41] J. C. Winter, F. Krauss, and G. Soff, Eur. Phys. J. C **36**, 381 (2004).
[42] Q. B. Xie and X. M. Liu, Phys. Rev. D **38**, 2169 (1988).
[43] Q. B. Xie, in *Proceedings of the 19th International Symposium on Multiparticle Dynamics*, Arles, France, 1988, edited by D. Schiff and J. Tran Thanh Vann (World Scientific, Singapore, 1988), p. 369.
[44] Z. T. Liang and Q. B. Xie, Phys. Rev. D **43**, 751 (1991).
[45] Q. Wang and Q. B. Xie, Phys. Rev. D **52**, 1469 (1995).
[46] Q. Wang and Q. B. Xie, J. Phys. G **21**, 897 (1995).
[47] J. Q. Zhao, Q. Wang, and Q. B. Xie, Sci. Sin. A **38**, 1474 (1995).
[48] Q. Wang, X. M. Liu, and Q. B. Xie, High Energy Phys. Nucl. Phys. **19**, 281 (1995).
[49] Q. Wang, Z. G. Si, and Q. B. Xie, Int. J. Mod. Phys. A **11**, 5203 (1996).
[50] Q. Wang, Q. B. Xie, and Z. G. Si, Phys. Lett. **B388**, 346 (1996).
[51] Z. G. Si, Q. B. Xie, and Q. Wang, Commun. Theor. Phys. **28**, 85 (1997).
[52] Z. G. Si and Q. B. Xie, High Energy Phys. Nucl. Phys. **23**, 445 (1999).
[53] Q. Wang, G. Gustafson, and Q. B. Xie, Phys. Rev. D **62**, 054004 (2000).
[54] Q. Wang, G. Gustafson, Y. Jin, and Q. B. Xie, Phys. Rev. D **64**, 012006 (2001).
[55] S. Y. Li, F. L. Shao, Q. B. Xie, and Q. Wang, Phys. Rev. D **65**, 077503 (2002).
[56] F. L. Shao, Q. B. Xie, S. Y. Li, and Q. Wang, Phys. Rev. D **69**, 054007 (2004).
[57] R. L. Jaffe, SLAC-PUB-1774, 1976 (unpublished).
[58] D. Strottman, Phys. Rev. D **20**, 748 (1979).
[59] D. Diakonov, V. Petrov, and M. V. Polyakov, Z. Phys. A **359**, 305 (1997).
[60] B. Wu and B. Q. Ma, Phys. Lett. **B586**, 62 (2004).
[61] B. Wu and B. Q. Ma, Phys. Rev. D **69**, 077501 (2004).
[62] Y. R. Liu, A. Zhang, P. Z. Huang, W. Z. Deng, X. L. Chen, and S. L. Zhu, Phys. Rev. D **70**, 094045 (2004).
[63] T. Nakano *et al.* (LEPS Collaboration), Phys. Rev. Lett. **91**, 012002 (2003).
[64] V. V. Barmin *et al.* (DIANA Collaboration), Phys. At. Nucl. **66**, 1715 (2003) [Yad. Fiz. **66**, 1763 (2003)].
[65] S. Stepanyan *et al.* (CLAS Collaboration), Phys. Rev. Lett. **91**, 252001 (2003).
[66] A. Airapetian *et al.* (HERMES Collaboration), Phys. Lett. **B585**, 213 (2004).
[67] V. Kubarovsky *et al.* (CLAS Collaboration), Phys. Rev. Lett. **92**, 032001 (2004); **92**, 049902(E) (2004).
[68] B. Aubert *et al.* (BABAR Collaboration), arXiv:hep-ex/0408037.
[69] R. L. Jaffe, Phys. Rev. D **17**, 1444 (1978).
[70] R. L. Jaffe, Phys. Rev. Lett. **38**, 195 (1977); **38**,617(E) (1977).
[71] A. J. Buchmann, G. Wagner, K. Tsushima, L. Y. Glozman, and A. Faessler, Prog. Part. Nucl. Phys. **36**, 383 (1996).
[72] A. J. Buchmann, G. Wagner, and A. Faessler, Phys. Rev. C **57**, 3340 (1998).
[73] F. Wang, J. I. Ping, D. Qing, and T. Goldman, arXiv:nucl-th/0406036.
[74] H. R. Pang, J. I. Ping, L. Z. Chen, F. Wang, and T. Goldman, Phys. Rev. C **70**, 035201 (2004).
[75] Z. Y. Zhang, Y. W. Yu, and X. Q. Yuan, Nucl. Phys. **A670**, 178 (2000).
[76] Q. B. Li, P. N. Shen, Z. Y. Zhang, and Y. W. Yu, Nucl. Phys. **A683**, 487 (2001).
[77] Y. W. Yu, P. Wang, Z. Y. Zhang, C. R. Ching, T. H. Ho, and L. Y. Chu, Phys. Rev. C **66**, 015205 (2002).
[78] Z. Y. Zhang, Y. W. Yu, P. N. Shen, L. R. Dai, A. Faessler, and U. Straub, Nucl. Phys. **A625**, 59 (1997).
[79] S. Pal, C. M. Ko, and Z. Y. Zhang, arXiv:nucl-th/0107070.

[80] Z. Y. Zhang, Y. W. Yu, C. R. Ching, T. H. Ho, and Z. D. Lu, Phys. Rev. C **61**, 065204 (2000).
[81] M. Hofmann, M. Bleicher, S. Scherer, L. Neise, H. Stocker, and W. Greiner, Phys. Lett. **B478**, 161 (2000).
[82] W. Hofmann, Annu. Rev. Nucl. Part. Sci. **38**, 279 (1988).
[83] A. Casher, H. Neuberger, and S. Nussinov, Phys. Rev. D **20**, 179 (1979).
[84] A. Casher, H. Neuberger, and S. Nussinov, Phys. Rev. D **21**, 1966 (1980).
[85] H. Scheck, Nucl. Phys. (Proc. Suppl.) **B1**, 291 (1988).
[86] R. Nouicer *et al.* (PHOBOS Collaboration), arXiv:nucl-ex/0208003.
[87] S. S. Adler *et al.* (PHENIX Collaboration), Phys. Rev. Lett. **91**, 072301 (2003).
[88] T. Sjostrand, L. Lonnblad, S. Mrenna, and P. Skands, arXiv:hep-ph/0308153.
[89] J. Randrup, Phys. Rev. C **68**, 031903 (2003).
[90] J. Letessier, G. Torrieri, S. Steinke, and J. Rafelski, Phys. Rev. C **68**, 061901 (2003).
[91] L. W. Chen, V. Greco, C. M. Ko, S. H. Lee, and W. Liu, Phys. Lett. **B601**, 34 (2004).
[92] F. M. Liu, H. Stoecker, and K. Werner, Phys. Lett. **B597**, 333 (2004).
[93] M. Bleicher, F. M. Liu, J. Aichelin, T. Pierog, and K. Werner, Phys. Lett. **B595**, 288 (2004).
[94] J. Schaffner-Bielich, R. Mattiello, and H. Sorge, Phys. Rev. Lett. **84**, 4305 (2000).
[95] J. Schaffner-Bielich, C. Greiner, A. Diener, and H. Stocker, Phys. Rev. C **55**, 3038 (1997).